Inorganica Chimica Acta 579 (2025) 122587

Contents lists available at ScienceDirect

Inorganica Chimica Acta

journal homepage: www.elsevier.com/locate/ica

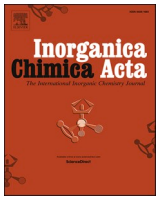

Reversible deprotonation as crucial step in bispidine copper-catalyzed aziridination reaction

Thomas Josephy [b], Markus Heiduk [a], Tobias Saxl [b], Katharina Bleher [a,b,*]

[a] Institute of Functional Interfaces, Karlsruhe Institute of Technology, Hermann-von-Helmholtz-Platz 1, 76344, Eggenstein-Leopoldshafen, Germany
[b] Universität Heidelberg, Anorganisch-Chemisches Institut, INF 270, D-69120 Heidelberg, Germany

ARTICLE INFO

Keywords:
Copper catalyzed aziridination
Bispidine
Deprotonation of copper(II)-amines
Nitrene character

ABSTRACT

Copper nitrene complexes are highly reactive species and known as active intermediates in copper-catalyzed C-H amination and aziridination. In this study, we investigated the reaction mechanism of a bispidine-based copper complex with a secondary amine in the selective aziridination of styrene using [N-(p-toluenesulfonyl)imino] phenyliodinane as oxidant. It was demonstrated that the addition of Et_3N to the reaction mixture facilitates a reversible deprotonation throughout the catalytic cycle, contributing to an overall accelerated product formation. Additionally, the use of two pentadentate ligands with secondary amines in combination with two tertiary methyl-amine ligands showed that the positioning of the secondary amine trans to the nitrene group is crucial for observing an increase of the turnover frequency. Furthermore, through the addition of radical quenchers and the investigation of additional substrates, a copper(II) radical nitrene intermediate was postulated, which concludes substrate conversion via a stepwise reaction mechanism.

1. Introduction

The construction of C-N structural motifs is one of the most important chemical transformations in synthetic organic chemistry. [1] Therefore, the development of efficient methods to construct these are of great interest. [2] One possibility for the formation of C-N bonds is the use of transition metal complexes that can catalyze aziridinations or aminations, through the formation of a nitrene-metal intermediate. [3–6] For this type of reaction, especially for aziridinations, copper complexes are the most extensively studied transition metal compounds. Since Evans et. al. intensively studied the copper-catalyzed aziridination with [N-(p-toluenesulfonyl)imino]phenyliodinane (PhINTs) [7–9] numerous ligand systems have been investigated for optimization. Additionally, various other metals such as manganese, cobalt, iron and ruthenium are also being investigated, alongside with metal-free conversions. [10–20] Due to the wide range of different ligands that have been studied, various reaction mechanisms have been reported. The main differences between the individual reaction mechanisms are primarily the oxidation state of the copper central atom, which varies from +I to +III, and whether the aziridine formation involves a concerted or a stepwise mechanism. [12,21,22] In this context, the question of the oxidation state of the copper central atom is closely linked to the electronic structure of the formed copper-NR active species. The proposed reaction mechanisms for the bispidine-based system studied here is shown in Fig. 1. [23]

Due to the electronic structure of the NTs group with six electrons in the valence shell of the nitrogen atom, the copper-NTs complex can exist in two different forms. Either in a singlet nitrene form (Fischer-type), where the two free electrons on the nitrogen atom lie in the same p-orbital, thus leaving an unoccupied vertically positioned p-orbital on the nitrogen, or in a triplet nitrosyl radical form (radical Fischer-type), where the two electrons are localized in each of the two available p-orbitals. [19,24,25] The two nitrene forms differ in their donor strength. The singlet form leads to a strong σ-donation, pushing electron density from the nitrene group into the d_{z2}-orbital of the copper central atom and to a π-backbonding, whereby electron density from the d_{yz}-orbital of the copper atom is directed into the unoccupied p-orbital of the nitrene group. The singlet form can thus be described by a double bond between the nitrene group and the copper central atom. In the triplet form, the σ-bond results from one of the two unpaired electrons on the nitrogen donor and an electron from the copper central atom. In this case no electron density is pushed from the nitrogen donor into the copper's d_{z2}-orbital but decreased by the contribution to the σ-bond formation. The second non-involved electron of the nitrogen

* Corresponding author.
E-mail address: katharina.bleher@kit.edu (K. Bleher).

https://doi.org/10.1016/j.ica.2025.122587
Received 3 September 2024; Received in revised form 23 December 2024; Accepted 5 February 2025
Available online 7 February 2025

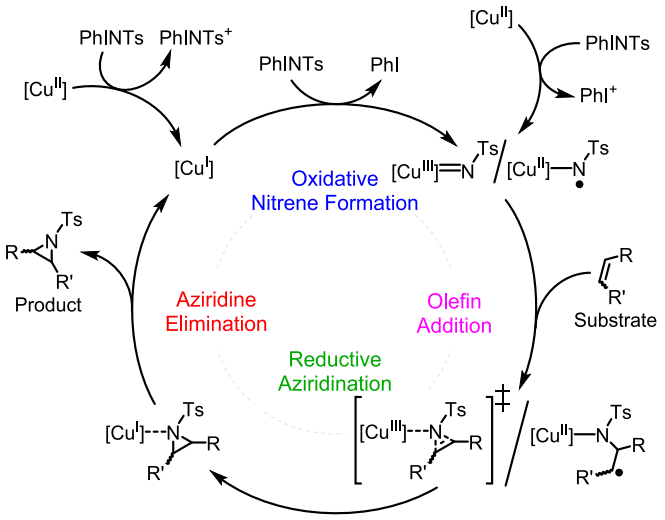

Fig. 1. Currently postulated reaction mechanism for the copper-bispidine catalyzed aziridination of alkenes with a copper(I) active species. Reprinted from [23] with permission from Elsevier.

atom is localized on the nitrene group as a radical. Here, the radical cannot form an additional π-bond with the d_{yz}-orbital as the orbital is already fully occupied in the d^9-electron configuration of the copper(II) central atom, thus the bond is weaker than in the singlet form. The triplet form is therefore described as a radical species with a single bond between the copper central atom and the nitrene group. Due to the electronic structure, the triplet species is typically linked to a stepwise mechanism in aziridine formation, while the singlet state has often been associated with a concerted pathway. [2,20,21,26–29]

In a recent study, we published a series of modified bispidine copper complexes, one with a secondary amine at N^3 (see Fig. 2 for atom numbering in bispidines) in trans-position to the NTs group. This complex exhibited an approximately 380-fold higher turnover frequency (TOF) compared to a comparable complex with a (methyl substituted) tertiary amine and achieved more than double the yield. In this study, we had already demonstrated that it is possible to reversibly deprotonate the acetonitrile-copper(II) complex using Et_3N, postulating that this is the basis for the increased reactivity exhibited by this complex in the catalysis. [23] Generally, deprotonation steps are common processes in for example zinc based enzymes, where a co-ligand is deprotonated for activation, or in Type-III copper enzymes, where a substrate is deprotonated by an amino acid residue to enable the reaction to proceed. [30,31] Based on this, we suspect that in the bispidine system

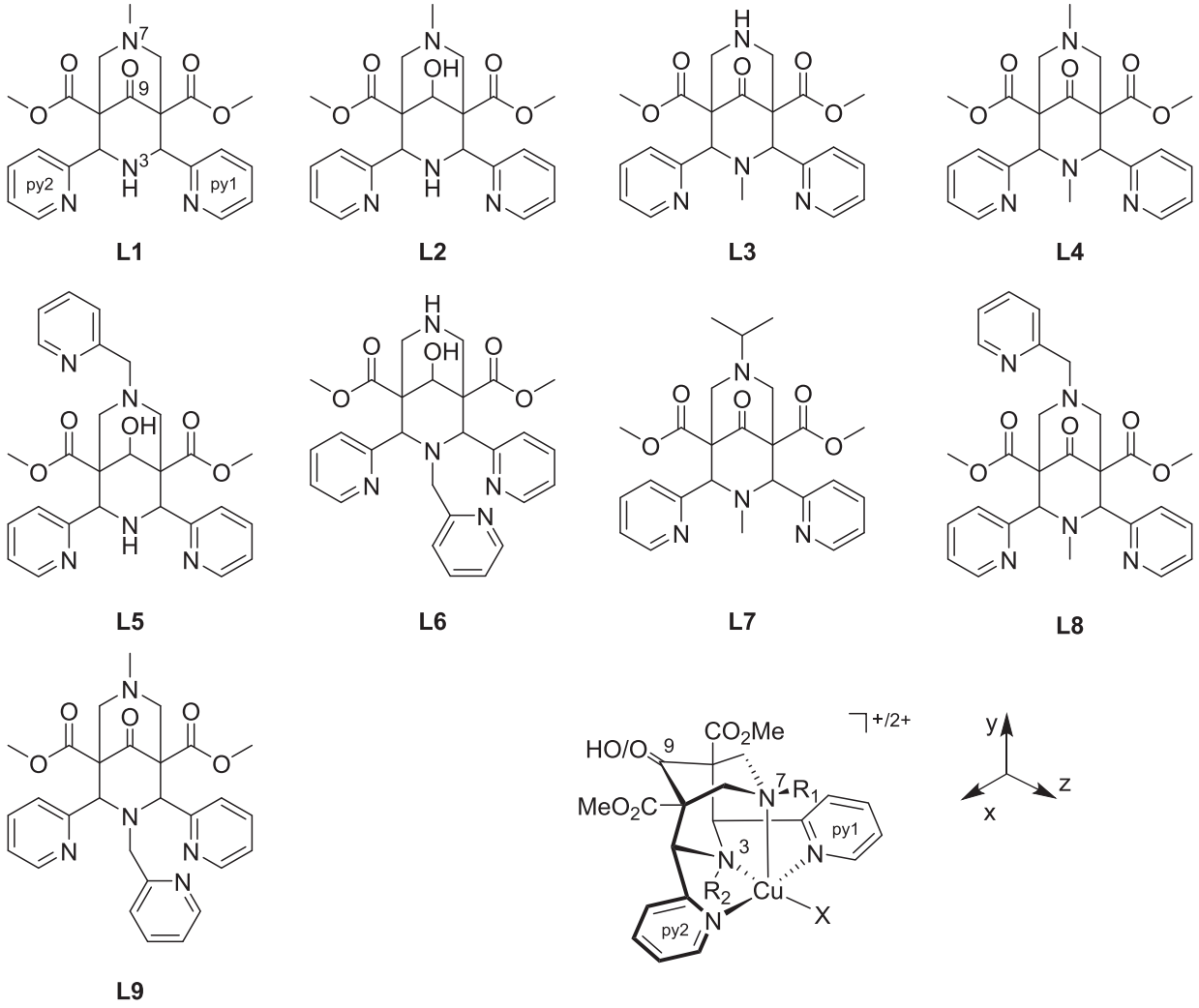

Fig. 2. Ligands used in this work. Numbering of atoms exemplarily explained with L1. In the right corner the coordination of the copper complex with a tetradentate ligand is shown (X = solvent/anion/NTs group).

under investigation, deprotonation at the amine can have a strong effect on reactivity, too.

In the present study, we conducted further experiments to substantiate the reversible deprotonation as crucial step also during the catalytic cycle.

2. Experimental Section

2.1. Materials and methods

All chemicals and reagents were purchased from commercial sources (ABCR; ACROS; Sigma-Aldrich; TCI). Dry solvents were used without further purification. Absolute acetonitrile was used from a solvent purification system MB SPS 5 from Braun. Deuterated solvents for NMR spectroscopy were purchased from Deutero. Styrene was degassed and stored over molecular sieves (4 Å) at −30 °C under argon in a Labmaster 130 (1250/780) glovebox from mBraun. Preparation and handling of air sensitive materials were carried out in a glovebox under argon or using standard Schlenk techniques. All Data were analyzed and visualized using OriginPro 2021b, unless otherwise stated.

ESI-MS experiments for characterization of the copper(II) complexes with L1-L4 and L7-L9 carried out on a ApexQe hybrid 9.4 T FT-ICR from Bruker by the Mass Spectrometry Facility, Department of Chemistry, University of Heidelberg, Heidelberg, Germany.

ESI-MS experiments for characterization of the copper complexes with L5 and L6 were carried out on a SCIEX qTOF 6600+ and experiments with added Et_3N, HOTf and PhINTs were carried out on a SCIEX X500R.

NMR spectra were recorded at 400 MHz (1H) and 101 MHz (13C) on an Advance II and at 600 MHz (1H) and 151 MHz (13C) on an Advance III from Bruker with the solvent as internal reference.

Elemental analyses were performed on a CHN-O Vario EL by the "Mikroanalytisches Labor", Department of Chemistry, Heidelberg University, Heidelberg, Germany.

UV/vis-NIR spectra of the Cu(II) precursors in Fig. S2 were recorded on an Agilent 8453 spectrophotometer equipped with a USP-203-A cryostat from Unisoku. Spectra of the complexes with L1-L3 in Fig. 4 were recorded using a V-570 spectrometer from Jasco. The measurements were carried out under temperature control in quartz cuvettes. All other spectroscopic investigations in the UV/vis-NIR range were conducted using a Genesys UV–visible spectrometer from Thermo Scientific in PMMA semi-micro disposable cuvettes. The data analysis was performed using OriginPro 2021. The data were smoothed using the Savitzky-Golay function (points of window = 20, polynomial order = 2), which reduces outliers and random variations while retaining the original shape.

For the electrochemical measurements, a 660D Electrochemical Workstation from CH Instruments with a three-electrode setup consisting of a glassy carbon working electrode (PFCE 3), a Pt wire as counter electrode, and an $Ag/AgNO_3$ reference electrode (0.01 M Ag^+, 0.1 M $(Bu_4N)^+(PF_6)^-$ in MeCN) was used. The measurement solutions were purged with argon and the measurement itself was carried out under argon atmosphere. A scan rate of 0.1 V/s was used. The redox potentials are reported with respect to fc/fc^+.

X-ray crystallography was performed on a Bruker D8 Venture diffractometer (details see Supporting Information). Plots of the crystal structures shown in this publication were performed using the program Olex2 (https://doi.org/10.1107/S0021889808042726). Crystallographic data for the structures reported in this paper have been deposited with the Cambridge Crystallographic Data Centre as supplementary publication no. CCDC with the deposition Numbers 2,380,886 (for CuL5) and 2,380,881 (for CuL6). These data can be obtained free of charge from The Cambridge Crystallographic Data Centre via www.ccdc.cam.ac.uk/structures.

2.2. Syntheses

Ligands L1-L9 and corresponding copper complexes were synthesized after literature-known procedures (Note: All copper complexes have already been published, except for the complexes with L5 and L6. The corresponding ligands have so far been reported as intermediates in the synthesis of other ligands. The complex syntheses were carried out according to the referenced literature.) [23,32–37] The oxidant [N-(p-toluenesulfonyl)imino]phenyliodinane (PhINTs) was synthesized according to the procedures of Yamada et al. and Evans et al., washed with dichloromethane and stored in a glovebox at −30 °C under argon until its use. [8,9,38]

General synthesis of the copper(II) complexes: The corresponding ligand and an equimolar amount of copper(II) trifluoromethanesulfonate were dissolved in acetonitrile or methanol to obtain an intense blue 0.5 to 2 mM solution. The mixture was stirred for 30 min at rt. for complete complexation. The complexes were obtained by ether diffusion at 4 °C as blue crystals in almost quantitative yields (90 to 98 %).

$[Cu^{II}L1(H_2O)](OTf)_2$. Elemental Analysis ($C_{24}H_{26}CuF_6N_4O_{12}S_2$ x 1.5 H_2O × 0.5 MeCN) [%], calc: C, 35.26; H, 3.61; N, 7.40; found: C, 35.07; H, 3.69; N, 7.45. ESI-MS (pos., MeOH) *m/z*: 654.0654 (100 %) $[Cu^{II}L1 + OTf + H_2O]^+$ (calc: 654.0663).

$[Cu^{II}L2(MeCN)](OTf)_2$. Elemental Analysis ($C_{26}H_{29}CuF_6N5O_{11}S_2$ x 0.5 H_2O × 0.5 MeCN) [%], calc: C, 37.76; H, 3.70; N, 8.97; found: C, 37.90; H, 3.95; N, 8.84. ESI-MS (pos., MeOH) *m/z*: 638.0718 (74 %) $[Cu^{II}L2 + OTf + H_2O]^+$ (calc: 638.0714),) m/z: 1425.0977 (100 %) $[2\ Cu^{II}L2 + 3\ OTf]^+$ (calc: 1425.0954).

$[Cu^{II}L3(MeCN)](OTf)_2$. Elemental Analysis ($C_{24}H_{26}CuF_6N_4O_{12}S_2$ x 2 H_2O × 0.5 MeCN) [%], calc: C, 34.89; H, 3.69; N, 7.32; found: C, 34.85; H, 3.63; N, 7.35. ESI-MS (pos., MeOH) *m/z*: 654.0663 (100 %) $[Cu^{II}L3 + OTf + H_2O]^+$ (calc: 654.0663).

$[Cu^{II}L4(MeCN)](OTf)_2$. Elemental Analysis ($C_{27}H_{29}CuF_6N_5O_{12}S_2$) [%], calc: C, 38.79; H, 3.52; N, 8.64; found: C, 38.74; H, 3.76; N, 8.64. ESI-MS (pos., MeOH) *m/z*: 550.1486 (79 %) $[Cu^{II}L4 + OMe + H_2O]^+$ (calc: 550.1483), 668.0824 (100 %) $[Cu^{II}L4 + OTf + H_2O]^+$ (calc: 668.0820).

$[Cu^{II}L5(MeCN)](OTf)_2$. Elemental Analysis ($C_{31}H_{32}CuF_6N_6O_{11}S_2$) [%], calc: C, 41.08; H, 3.56; N, 9.27; found: C, 41.14; H, 4.10; N, 9.05. ESI-MS (pos., MeCN/H_2O 50:50) *m/z*: 283.0748 (100 %) $[Cu^{II}L5]^{2+}$ (calc: 283.0727), 565.1394 (70 %) $[Cu^{II}L5_{-H+}]^+$ (calc: 563.1381), 715.1005 (53 %) $[Cu^{II}L5 + OTf^-]^+$(calc: 715.0979).

$[Cu^{II}L6(H_2O)](OTf)_2$. Elemental Analysis ($C_{29}H_{31}CuF_6N_5O_{12}S_2$) [%], calc: C, 39.44; H, 3.54; N, 7.93; found: C, 39.33; H, 3.69; N, 8.07. ESI-MS (pos., MeCN/H_2O 50:50) *m/z*: 611.1412 (100 %) $[Cu^{II}L6 + OAc^-]^+$ (calc: 611.1436).

$[Cu^{II}L7(H_2O)](OTf)_2$. Elemental Analysis ($C_{27}H_{32}CuF_6N_4O_{12}S_2$ x 0.25 H_2O) [%], calc: C, 38.56; H, 3.85; N, 6.95; found: C, 38.45; H, 4.14; N, 7.00. ESI-MS (pos., MeOH) m/z: 578.1801 (100 %) $[Cu^{II}L7 + OMe + H_2O]^+$ (calc: 578.1796), 696.1142 (77 %) $[Cu^{II}L7 + OTf + H_2O]^+$ (calc: 696.1133).

2.3. Aziridination reactions

Standard conditions: In a glove box, a 1.5 mL glass vial was equipped with a stirring bar, 1 eq PhINTs (10 to 25 mg, 27–67 μmol) and 5 eq styrene (10 to 40 μL, 88–350 μmol). The reaction was started by adding a 5 mM solution of the corresponding copper complex (0.05 eq), dissolved in dry, absolute acetonitrile. The vial was closed and placed as fast as possible (20 to 30 s) on a stirrer. The reaction duration was obtained by monitoring the reaction mixtures. Due to the poor solubility of the oxidant in MeCN the moment the solution becomes clear is equal to the end of the reaction. For the determination of the catalytic yields, the reactions were stirred for 18 to 24 h in total, but at least until a clear solution was obtained. The vials were taken out of the glove box and the solutions were filtered over a silica pipette column to separate the

copper catalysts. The columns were washed with 5 to 10 mL ethyl acetate and the combined filtrate was evaporated at 40 °C. The aziridination yields were determined by ^{1}H NMR spectroscopy. Therefore, 1,3,5-trimethoxybenzene (8 to 20 mg – exact amount was noted) was added as internal standard to the residue which was dissolved in $CDCl_3$. All experiments were performed twice (if a deviation of max 5 % was obtained), else the experiments were repeated a third time. The detailed determination of yield is described in the SI.

Under oxygen/air: Reactions in air are set up under standard conditions. The oxidizing agent was weighed into a 1.5 mL vial in the glovebox. The respective copper solution was also prepared in the glovebox and then taken out. The reaction was set up and carried out as described in the standard conditions. For reactions under oxygen atmosphere, the respective copper solution was also prepared in the glovebox, and the oxidizing agent was weighed into a 1.5 mL vial in the glovebox. After removal from the glovebox, the vial was flushed with oxygen, and the copper solution was bubbled with oxygen for 2 min. After combining the reaction components, the reaction mixture was bubbled with oxygen for another 2 min. The vial was then sealed and stirred until the reaction was complete.

With radical quenchers: Experiments were conducted with the radical quenchers BHT and TEMPO. The reactions were carried out as described under standard conditions, but after weighing the oxidizing agent, the solid radical quencher was also added to the vial. The substrate was added subsequently, and the reaction was initiated by adding the copper solution. The equivalents were chosen to achieve a 1:20:20:100 molar ratio of Cu-catalyst: oxidant: radical quencher: substrate.

With alternative substrates: Experiments with cis-stilbene/trans-β-methylstyrene were carried out exactly as described under standard conditions, except that the corresponding substrate was used instead of styrene. The ratios of the individual components were not altered, nor was the order of substrate addition.

With base/acid: For the reactions with added base (Et_3N) or acid (HOTf), solutions in acetonitrile were prepared at concentrations of 1.34 M, 0.67 M, and 0.134 M. Catalyzes were carried out under standard conditions. However, after weighing the oxidizing agent and adding the substrate, 10 μL of the corresponding solution was pipetted in, and the reaction was immediately initiated by adding the Cu solution. The amounts added correspond to 0.5 eq, 1 eq or 10 eq of acid or base relative to the amount of copper catalyst.

3. Results and discussion

3.1. Synthesis and characterization of $[Cu^{II}L5/L6]^{2+}$ complexes

Ligands L5 [39] and L6 [40] were synthesized after literature-known procedures. These ligands were chosen to specifically block the transposition of the secondary amine with an additional pyridine donor of the ligand, thus preventing the coordination of the nitrene group trans to the secondary amine. The corresponding copper(II) complexes were synthesized by mixing the copper(II) triflate salt with ligand in equimolar amounts in MeCN, which leads to instant formation of deep blue complex solutions. Subsequently, the complexes were characterized using UV/vis-NIR and CV (see Table 2). While no trend is observed in the absorption maxima between tetra- and penta-coordinated complexes, the values in the CV measurements, at −686 mV and − 694 mV vs fc/fc^+ for $[CuL5]^{2+}$ and $[CuL6]^{2+}$, are in a similar range as the complexes with the pentadentate ligands L8 (−690 mV) and L9 (−576 mV), whereas the redox potentials for the complexes with tetradentate ligands are significantly higher (−395 to −516 mV). This implies complete coordination of all donors of the ligand in solution. The difference in potentials between $[CuL6]^{2+}$ and $[CuL9]^{2+}$ can be explained by the reduced backbone at C^9. It was shown that this can lead to a reduction of the redox potential of up to 100 mV as observed with different transition metals and again demonstrated with $[CuL1]^{2+}$ and $[CuL2]^{2+}$. [32,41–44] Additionally the full complexation was confirmed by the crystal structures of the two complexes $[Cu^{II}L5]^{2+}$ and $[Cu^{II}L6]^{2+}$; the required crystals were obtained by slow evaporation of the solvent (see Fig. 3). Relevant parameters of the obtained structures and for complexes shown in Fig. 2 are listed in Table 1. The distances between the donor atoms and the central atom vary significantly between the complexes, which is mainly due to the different co-ligands (MeCN, Cl^-) and also the previously mentioned reduction of the C^9 ketone, which can lead to significant electronic changes. Notably, the structural parameters of the complex with L6 stand out. Here, as with the analogous complex with L9, the elongated pseudo Jahn-Teller axis has rotated from the N^7-Cu axis to the py1-Cu-py2 axis, which is particularly evident in the increased distance between the two pyridines, py1 and py2. This is, however, known for copper bispidine complexes with isomers of this pentadentate ligand, and it can be assumed that elongation along the N^7 axis also occurs in solution, as the minima of the individual bond-stretch

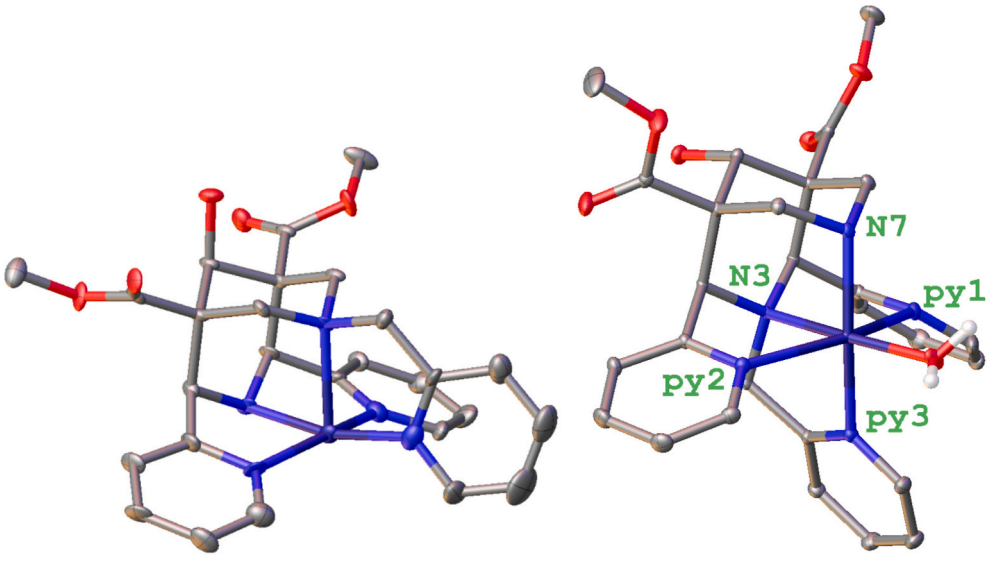

Fig. 3. Olex2 plots of the crystal structure analyses of the copper(II) complexes with ligands L5 (left) and L6 (right) with a co-ligand trans to N^3 (water), respectively. Counter ions, H-atoms (except on water co-ligand) and co-crystallized solvent molecules are omitted for clarity, ellipsoids are shown at 50 % probability level. Colour code: blue: N, red: O, dark blue: Cu, grey: C. (For interpretation of the references to colour in this figure legend, the reader is referred to the web version of this article.)

Table 1
Selected bond lengths and angles of the crystal structures of relevant bispidine copper(II) complexes ($[Cu^{II}LnX]^{m+}$) with distances given in (Å) and angles in (°); see Supporting Information for details.

$Cu^{II}LX$ (Å)/(°)	Cu-N^3	Cu-N^7	Cu-X/Y	X/Y	Cu-py1	Cu-py2	py1-Cu-py2	N^3-Cu-X	N^3-Cu-N^7	Lit
L1	2.007 (2)	2.358 (2)	2.228 (6) /	Cl^-/	2.013 (2)	2.009 (2)	4.022	4.235	81.25 (6)	[49]
L2	2.005 (2)	2.346 (2)	2.235 (9) /	Cl^-/	2.023 (2)	2.019 (2)	4.042	4.240	81.41 (6)	[49]
L3	2.018 (3)	2.242 (3)	1.953 (4) /	MeCN /	2.005 (4)	2.006 (4)	4.011	3.971	84.92 (12)	[23]
L4	2.022 (2)	2.353 (2)	1.972 (2) / 2.757 (2)	MeCN / ClO_4^-	1.994 (2)	2.003 (2)	3.997	3.994	83.26 (2)	[32]
L5	2.0013 (2)	2.2796 (2)	1.9766 (2) /	py /	2.0103 (2)	2.0145 (2)	3.9544	3.9493	84.4 (10)	This work
L6	2.0486 (13)	2.0189 (13)	1.9687 (12) / 2.0030 (14)	H_2O / py	2.3566 (13)	2.6020 (14)	4.8021	4.0107	87.19 (5)	This work
L8*	2.036 (2)	2.368 (2)	2.029 (2) / 2.717 (−)	py / Cl	2.028 (2)	2.029 (2)	4.057	4.065	82.53 (6)	[50]
L9	2.105 (2)	2.082 (3)	2.015 (2) / 2.027 (−)	MeCN / py	2.353 (2)	2.260 (2)	4.613	4.120	86.44 (−)	[45]

* C9 hydrolyzed.

isomers are close to each other and are part of a flat potential-energy surface with multiple shallow minima, resulting from the rigid but flexible bispidine backbone. [45] As indicated through the redox potentials, also the crystal structures show full coordination of the ligands to the copper center. The corresponding fivefold coordination for $[CuL5]^{2+}$ and sixfold coordination for $[CuL6]^{2+}$ is further confirmed by the UV/vis-NIR spectra, where the low-energy band between 900 and 950 nm, corresponding to the transition from the d_{z2} to the d_{x2-y2}orbital in square pyramidal coordination, is absent in $[CuL6]^{2+}$ (see Table 2). [46–48]

3.2. Catalytic experiments

In the following, we tested various influences in the catalyzed aziridination reaction with PhINTs and styrene to draw conclusions about the reaction mechanism and to more closely examine the impact of the introduced secondary amines.

We first repeated the catalyzes for complexes with L1, L5, L6 and L7 under the reaction conditions as described by Bleher et al. [23] This means that the reactions were conducted in a ratio of 1:20:100 cat: ox: styrene in MeCN with a copper complex concentration of 5 mM at room temperature under argon. In Table 2, the results of the catalyzes with all ligands from Fig. 2 are listed.

In our publication from 2022 we found that the complexes with ligands containing a secondary amine in position N^3 increase the TOF by approximately 380-fold, in comparison to complexes with analog ligands containing methyl substituted tertiary amine at N^3. In contrast the substitution of the tertiary amine at N^7 only led to an increase of approximately 5-fold. We concluded that the key reason is the relative positioning of the secondary amine to the nitrene group, which can either be in trans- or cis-position and thus significantly differ in its influences on the properties of the nitrene. In tetradentate bispidines, the reactive group is typically positioned trans to N^3, [51] and this would also correspond to the observed results, indicating that only substitution of the alkyl group at N^3 leads to a significant increase in reactivity.

By synthesizing the ligands L5 and L6 which only provide one unoccupied coordination site in the complex, we force the nitrene group in the cis-position to the secondary amine, thus allowing us to investigate the effects of the positioning. When evaluating the parameters, it must be considered that the pentadentate bispidine derivatives are generally slower and yield lower outputs compared to the tetradentate bispidines. This is due not only to the increase in steric hindrance from the five-coordinated ligand, which reduces the accessibility of the copper central atom, but also to the fact that the redox potential is altered by the modified electronic environment, generally leading to lower potentials, which are in general associated with lower aziridination efficiency. [50,52] Comparing the pentadentate N^3H derivative $[Cu^{II}L5]^{2+}$ with its alkylated analogue $[Cu^{II}L8]^{2+}$, it is evident that both the yield (92 % vs. 22 %) and the TOF (67 h^{-1} vs. 1 h^{-1}) have increased drastically. In contrast only minor changes were obtained comparing the pentadentate N^7H derivative $[Cu^{II}L6]^{2+}$ and its alkylated analogue $[Cu^{II}L9]^{2+}$ (yield 63 % vs. 34 %, TOF 3 h^{-1} vs. 1 h^{-1}). Hence, the result of the N^7H derivative is similar to the observations for the complexes with tetradentate bispidines $[Cu^{II}L3]^{2+}$ (72 % yield, TOF 8.7 h^{-1}) and $[Cu^{II}L4]^{2+}$ (35 % yield. TOF 1.3 h^{-1}), the yield doubled, however, there was only a 3 to 5-fold increased TOF.

The exceptional behavior of $[Cu^{II}L5]^{2+}$ could be explained by an altered redox potential. Previous studies have shown a correlation between higher reactivities and yields and more positive redox potentials. [52] However, only a differences of 4 mV was found for the complexes with L5 and L8, and after deprotonation the redox potential becomes even more negative as demonstrated for $[Cu^{II}L1]^{2+}$. [23] It is more likely, that the secondary amine at N^3 influences the reaction occurring in a different manner. We suspect that the TOF in this complex rises to 67 h^{-1} because the coordination of the nitrene group can partially also occur trans to N^3H. However, the resulting TOF of this reaction is significantly lower compared to $[Cu^{II}L1]^{2+}$, as the coordinating pyridine donor of the ligand must first dissociate before the highly reactive nitrene species trans N^3 can be formed. The ability to deprotonate the secondary amine at position N^3 seems capable of weakening the donor in the trans-position, thereby promoting the dissociation of the additional pyridine donor and thus enabling the coordination of the oxidizing

Table 2
Yield in aziridination reactions with styrene (cat: PhINTs: styrene 1:20:100) in MeCN at rt. under argon atmosphere. Yields were measured after 18 h. Values are the mean values from duplicates. Values for absorption bands and redox potentials and yields were taken from [23], except values for $[Cu^{II}L5]^{2+}$ and $[Cu^{II}L6]^{2+}$.

Complex	E° (mV vs. fc/fc^+)	Λ max (nm) [ε (mol^{-1} L^{-1})]	Yield (%)	TOF (h^{-1})	Lit
L1	−395	691 (131) 913 (32)	81.5 ± 1.5	527 ± 14	[23]
L2	−514	623 (135) 925 (32)	81.0 ± 1.0	505 ± 27	[23]
L3	−516	637 (110) 977 (24)	71.5 ± 0.5	8.7 ± 0.5	[23]
L4	−504	626 (107) 899 (26)	35.0 ± 0.0	1.3 ± 0	[23]
L5	−686	635 (118) 955 (60)	91.9 ± 3.3	67 ± 0	This work
L6	−694	634 (77)	63.2 ± 2.4	3.0 ± 2.0	This work
L7	−415	617 (131) 892 (25)	66.5 ± 1.5	9.1 ± 0.2	[23]
L8	−690	629 (110) 959 (39)	22.0 ± 2.0	0.9 ± 0	[23]
L9	−576	664(74)	33.5 ± 0.5	1.4 ± 0	[23]
$Cu(OTf)_2$			70.5 ± 1.5	1371 ± 65	[23]

agent. This assumption is supported by three observations: First, the position trans to N^3 is the preferred coordination site for co-ligands in the bispidine system, as evident from the crystal structures of the copper (II) complexes with tetradentate bispidines and also from studies with iron(IV) oxido complexes. [23,51] Second, both complexes that direct the nitrene group in cis-position to the secondary amine ($[Cu^{II}L3]^{2+}$ and $[Cu^{II}L6]^{2+}$) show a TOF smaller than 10 per hour. Third, the behavior among the individual complexes is consistent, i.e., comparing the complex $[Cu^{II}L9]^{2+}$ with $[Cu^{II}L6]^{2+}$ shows the same trend as observed from $[Cu^{II}L3]^{2+}$ and $[Cu^{II}L4]^{2+}$— both TOF and yield approximately double. For $[Cu^{II}L5]^{2+}$, where only the cis-position is available without dissociation, similar results should therefore be expected, yet the complex with L5 shows approximately a 4-times increase in yield and a 70-folds increased TOF, compared to $[Cu^{II}L8]^{2+}$. Based on these results, further experiments were conducted to investigate the influence of deprotonation in more detail.

3.3. *Influence of varying reaction conditions on the reaction mechanism.*

Addition of Acid/Base It was already demonstrated that $[Cu^{II}L1]^{2+}$ can be reversibly deprotonated, as evidenced by significant reversible changes in the UV/vis-NIR spectrum (see Fig. 4). The same experiments were also conducted for $[Cu^{II}L2]^{2+}$ and $[Cu^{II}L3]^{2+}$ as well as for $[Cu^{II}L5]^{2+}$and $[Cu^{II}L6]^{2+}$. It is clearly visible that changes in the UV/vis-NIR spectrum occur for $[Cu^{II}L2]^{2+}$ after the addition of 10 eq of Et_3N, as reported for $[Cu^{II}L1]^{2+}$, but for $[Cu^{II}L3]^{2+}$ due to less pronounced changes in the UV/vis-NIR spectrum, no conclusions about possible deprotonation with Et_3N could be drawn. The same applies to the pentadentate complexes. For $[Cu^{II}L5]^{2+}$, a clear change in the spectrum is observed upon addition of the base, whereas no significant change is seen for the isomeric $[Cu^{II}L6]^{2+}$ complex. Additionally, in case of $[Cu^{II}L5]^{2+}$, the influence of the reduced backbone is evident, as the spectrum closely resembles that of $[Cu^{II}L2]^{2+}$. Since deprotonation is observed in both $[CuL2]^{2+}$ and $[CuL5]^{2+}$, attempts were made to determine their pKa values (see SI). Only by using a stronger base, pyrrolidine, the pKa value of $[CuL2]^{2+}$ was determined to be 21.75 ± 0.27 (under non-anhydrous conditions in MeCN). For comparison, the pKa value of $[CuL1]^{2+}$ was determined to be 18.35 ± 0.06 using triethylamine. The determination for $[CuL5]^{2+}$ was unsuccessful, as sufficient deprotonation was only achieved with a large excess of pyrrolidine, and the measurements were inconsistent. These results suggest that the pKa value of this amine group is higher as for $[CuL2]^{2+}$. For the N^7H derivatives, only minimal changes in the spectrum were observed upon the addition of Et_3N or pyrrolidine. For this reason, pKa value determination could not be carried out, but based on the changes in the UV/vis-NIR spectra we were able to sort the pKs values qualitatively ($[CuL1]^{2+}$ (18.35 ± 0.06) < $[CuL2]^{2+}$ (21.75 ± 0.27) ≤ $[CuL5]^{2+}$ < $[CuL3]^{2+}$ < $[Cul6]^{2+}$; see SI). Interestingly, when analyzing the pKa values and TOF, a correlation can be observed, where a lower pKa value of the secondary amine is associated with a higher TOF. However, more precise determination of the pKa values and additional data points would be necessary to confirm this connection definitively. To investigate whether $[Cu^{II}L3]^{2+}$ is also deprotonated under catalytic conditions, additional ESI-MS experiments were conducted. For this, complexes with the ligands L1, L3, and L4 were treated with an excess of PhINTs and were then measured to see if a deprotonated species was also present. Additionally, complex solutions with either 0.5 eq or 10 eq Et_3N were measured as reference. The corresponding mass spectra for $[Cu^{II}L3]^{2+}$ are shown in Fig. 5, and for the other complexes, the spectra are displayed in the Supporting Information. From the spectra it is clear that both the addition of base and PhINTs results in the observation of a deprotonated species at 486.0963 *m/z*. This is also the case for $[Cu^{II}L1]^{2+}$. As expected, no change occurs with $[Cu^{II}L4]^{2+}$ upon the addition of base or PhINTs. However, as shown in Fig. 5c, the intact copper nitrene species was detected in traces upon the addition of PhINTs. As a result from these experiments, it is concluded that both $[Cu^{II}L1]^{2+}$ and $[Cu^{II}L3]^{2+}$ can be deprotonated during the catalytic cycle of the aziridination of styrene with PhINTs.

To understand why the effect of deprotonation has such varying impacts depending on the ligand used, the interacting orbitals must be examined. In complexes with a secondary amine at N^3, the secondary amine interacts with the same orbitals of the copper central atom as the trans-positioned nitrene group (see Fig. 6). Both donors form a σ-bond with the d_{z2}-orbital of the copper central atom, pushing electron density into the same orbital and thus directly influencing each other. Deprotonation of the donor N^3 in trans-position to the nitrene group initially leads to an increased electron density at the N-donor and thus to a stronger electron donation ability, resulting in a higher electron density in the d_{z2}-orbital of the copper central atom. Additionally, at donor N^3, a fully occupied orbital containing a lone pair is now present, pushing electron density into the d_{yz}-orbital of the copper central atom. Deprotonation of a secondary amine in position N^3 thus leads to higher electron density in both orbitals interacting with the NTs group. In contrast, the cis-positioned donor N^7 forms its σ-bond with the d_{x2-y2}-orbital, pushing electron density into an orbital orthogonal to the nitrene group. Therefore, there is no direct interaction with the σ-bond of the NTs group. So, if the secondary amine in position N^7 is deprotonated, this has no direct influence on the Cu-NTs σ-bonding, although more electron density is pushed into the bonding orbital. But as with N^3, the deprotonation leads to a free pair of electrons at the donor N^7, located in a p-orbital perpendicular to the σ-bond. As for N^3 the lone pair pushes additional electron density into the d_{yz}-orbital by the deprotonation in

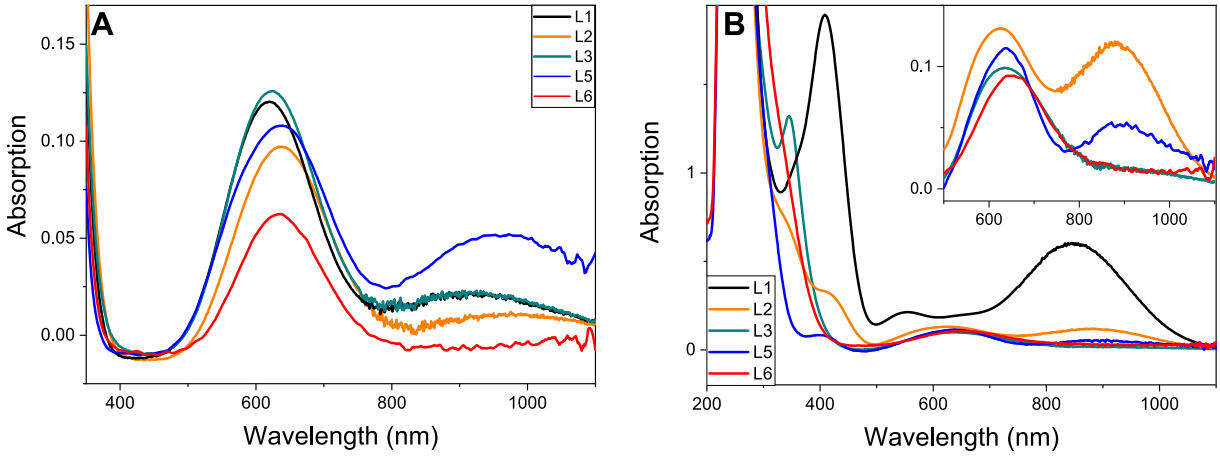

Fig. 4. UV/vis-NIR spectra of 1 mM copper(II) complex solutions in MeCN at rt. A: without base addition; B: with 10 eq Et_3N.

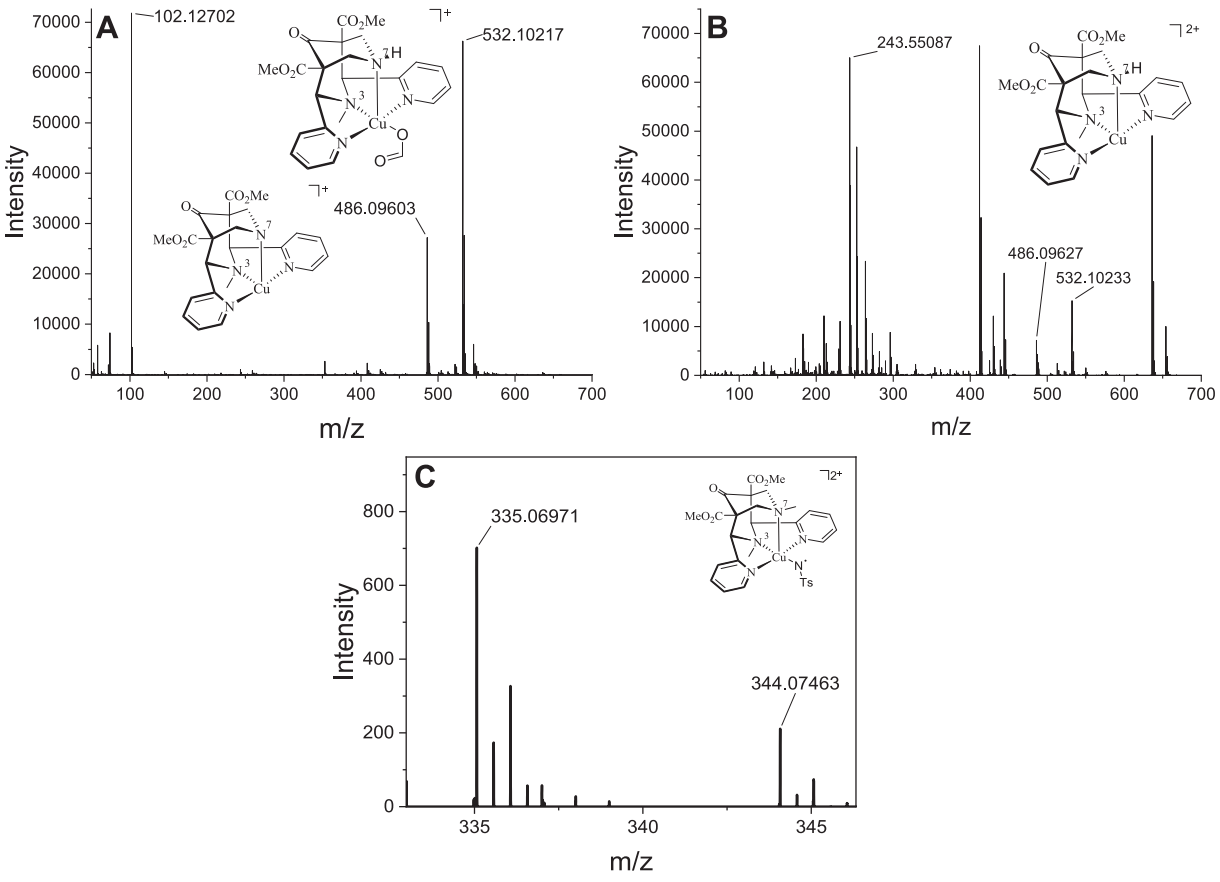

Fig. 5. HR-ESI-MS experiment of A: $[Cu^{II}L3]$ with 10 eq of Et_3N (102.1202 $[Et_3N + H^+]$; 486.0960 $[Cu^{II}L3_{-H+}]^+$; 532.1022 $[Cu^{II}L3 + FA^-]^+$; B: $[Cu^{II}L3]$ with excess PhINTs (additional signal 243.5509 $[Cu^{II}L3]^{2+}$. All additional signals that were identified, as well as spectra for the complexes $[Cu^{II}L1]^{2+}$and $[Cu^{II}L4]^{2+}$, are depicted in the Supporting Information).C: MS spectrum of $[Cu^{II}L4]^{2+}$ with an excess of PhINTs. The intact nitrene species is visible (335.0693; $[Cu = NTs\ L4]^{2+}$), as well with an additional water molecule (344.0746, $[Cu = NTs\ L4]^{2+}$ x H_2O).

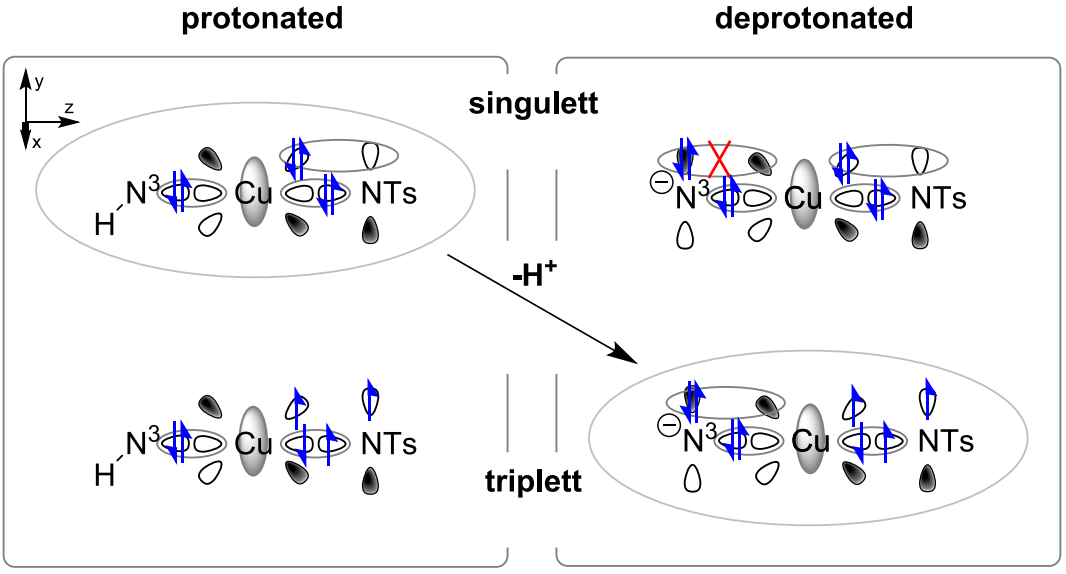

Fig. 6. Influence of the deprotonation of the N^3 donor on the electronic state of the nitrene complex. Shown are the orbitals relevant to bonding, including the electrons important for interactions. (N: sp^3 - protonated, $sp^2 + p_y$ - deprotonated, Cu: $d_{z2} + d_{yz}$, NTs: $sp^2 + p_y$). Orbitals that form a bond with each other are indicated by an ellipsoid, and repulsive interactions are marked with a red cross. (For interpretation of the references to colour in this figure legend, the reader is referred to the web version of this article.)

position N^7. However, this has only minor impact on the bond of the nitrene group and thus on its binding strength.

Comparing the two possible secondary amines and the consequences of deprotonation, it is noticeable that only a deprotonation in position N^3 could lead to a significant change in the nitrene character. Due to the higher electron density in the d_{z2}-orbital, the triplet form of the nitrene, with a weaker σ-bond, becomes energetically more favorable, while the singlet form, with a stronger σ-bond, becomes energetically less favorable (see Fig. 6). The radical character of the nitrene group is thus increased, and at the same time, the reactivity of the nitrene complex is enhanced.

To further support our concept and investigate the influence of the deprotonation on catalytic activity, we wanted to test the influence on the rate of the aziridination reaction by adding various equivalents of base or acid to the reaction mixture. The results of catalytic experiments with 0.5, 1, and 10 equivalents of added Et_3N in respect to the copper complex concentration are shown in Table 3.

Upon addition of 0.5 equivalents of Et_3N, we observe an increased TOF for all complexes studied. A particular significance is observed for $[Cu^{II}L1]^{2+}$. Here we found a 5-fold increase in TOF upon the addition of 0.5 and 1 eq Et_3N. (Note: The reaction duration was obtained by monitoring the reaction mixtures. Due to the poor solubility of the oxidant in MeCN the moment the solution becomes clear is taken as the end of the reaction. Due to the very rapid clarification of these reaction solutions, the recorded TOFs are associated with a large measurement error.) Regarding the yields with the addition of 0.5 and 1 equivalent of base, the values obtained remain comparable to experiments without added base. Only upon the addition of 10 equivalents of base a drastic decrease in yield is observed with all the complexes studied, along with a further accelerated TOF. The same trend is also observed when using pure copper(II) triflate as catalyst. These findings support our hypothesis upon the reversible deprotonation within the catalytic cycle, since the TOFs of the N^3H derivatives are disproportionately accelerated by the addition of moderate amounts of bases in comparison to the other complexes.

To explain the reduced yields upon the addition of 10 eq of Et_3N and to rule out that the formed product is unstable under those conditions, we synthesized the corresponding 2-phenyl-1-tosylaziridine [9] and mixed it with the same molar amount of Et_3N, then undertook the same work up as with the catalyzes (see SI for detailed results). Compared to the control (product without additional base, but also with subsequent workup), we observed a decrease of 10 %. However, this does not explain the collapse in yields observed in the catalytic experiments. Since we observe a high TOF and low yields across all samples, regardless of the type of ligand and including $Cu(OTf)_2$, it is questionable at high base concentrations whether the high TOF is solely due to deprotonation or whether additional effects, such as improved solubility of the oxidizing agent in MeCN, contribute to accelerating the reaction. Due to this, it is suspected that the decline in yields is caused by a faster occurring side reaction, such as polymerization, which consumes the oxidizing agent and making it unavailable for the aziridination causing the overall collapse of yields.

To test the counter effect, additional experiments were conducted with acid added, see Table 4. Here, the reaction is expected to slow down due to the lower pH, as the equilibrium is shifted away from the deprotonated species.

Considering the results with the addition of 0.5 eq and 1 eq of acid, it is initially observed that the TOF, especially for the complex $[CuL1]^{2+}$, drastically drops to 95 per hour. The same trend is also observed for the complex $[CuL2]^{2+}$, but as upon the addition of base the effect is less pronounced as for complex $[CuL1]^{2+}$. This could be due to the presence of a hydroxyl group on the backbone C^9, which could also be de−/protonated, thus somewhat mitigating the effect of the base and acid. Effects on the TOF are also observed in the complexes with L3 and L7, but these do not decrease as significantly as with the N^3H derivatives. It is evident that in the blind samples, as opposed to those without added acid, non-negligible amounts of product are formed. This is attributed to the acid used—since spectroscopically pure acid was not employed and the acid was extracted using metal cannulas for dilution, it is assumed that free metal ions are added to the reaction mixture, which can also catalyze this reaction. With the addition of 10 equivalents of acid this observation becomes highly visible as contrary to expectations the TOFs for all complexes increased. Where a decrease was previously observed, it is suspected that there is an overlap with the previously mentioned catalysis by free metal ions, resulting in an overall increase in the TOFs, most likely supported by further copper ions which were released from the complexes by the protonation of the ligands. Across all experiments, it was observed that the yield decreases with an increasing amount of acid added. Experiments in which the resulting product was treated with acid showed that 2-phenyl-1-tosylaziridine is not stable under those conditions (see SI). It is suspected that the three-membered ring is opened, leading to the disappearance of the corresponding NMR signals. However, due to the significantly slower TOF of the N^3H derivatives compared to the other complexes used, and in combination with the results of the added base, it confirms the suspicion that this complex derives its reactivity from a reversible deprotonation in the catalytic cycle.

Investigation of the oxidation state of the catalytically active species To gain further information about the reaction mechanism of $[CuL1]^{2+}$ a series of experiments under air and with actively added O_2 were conducted (see Table 5). In both cases a decline in yield and TOF can be observed. The TOF decreases significantly, while the yield is roughly halved. These results corroborate the hypothesis that the copper central atom needs to be in the oxidation state +I to exhibit catalytic activity. It shows also, that PhINTs is consumed for the reduction of the Cu(II) complex to the Cu(I) species and is therefore no longer available for catalytic conversion, resulting in a significant decrease in yield. [21,50,52] At the same time the significantly reduced TOF shows that less active species is available in the reaction solutions as Cu(I) gets easily re-oxidized by the oxygen.

Investigation of the copper nitrene character in the catalytic cycle To get insight into the nitrene character in the catalytic cycle, we have employed cis-stilbene as substrate in the aziridination reaction. As shown in Table 5, isomerization occurred with cis-stilbene, while no conformation change was observed with (*E*)-β-methylstyrene as reference substrate.

Table 3
Aziridination yields with different equivalents of added base Et_3N. (The increased yield in blind samples with base, was attributed to traces of transition metals in the base added, which are likely also capable of catalyzing the reaction to some extent.)

Complex	0 eq Et_3N		0.5 eq Et_3N		1 eq Et_3N		10 eq Et_3N	
	Yield (%)	TOF (h^{-1})	Yield (%)	TOF (h^{-1})	Yield (%)	TOF (h^{-1})	Yield (%)	TOF (h^{-1})
L1	81.8 ± 2.5	528 ± 6	87.9 ± 3.9	2426 ± 74	77.4 ± 1.1	2564 ± 164	10.7 ± 2.1	4152 ± 2327
L2	81.0 ± 1.0	505 ± 27	70.9 ± 5.3	679 ± 6	80.2 ± 11.4	874 ± 27	5.3 ± 1.0	1060 ± 31
L3	71.5 ± 0.5	8.7 ± 0.5	89.1 ± 0.8	17 ± 0	71.5 ± 0.3	17 ± 0	13.7 ± 7.1	759 ± 411
L7	61.9 ± 3.0	9.1 (lit)	65.1 ± 3.3	10 ± 0	70.6 ± 0.6	10 ± 0	9.1 ± 1.5	425 ± 65
$Cu(OTf)_2$	78.75	2667					8.5	1075
blind			15.5 ± 1.0	> 1			5.3 ± 3.9	1 ± 0

Table 4
Aziridination yields with different amounts of added acid HOTf.

Complex	0 eq HOTf		0.5 eq HOTf		1 eq HOTf		10 eq HOTf	
	Yield (%)	TOF (h^{-1})	Yield (%)	TOF (h^{-1})	Yield (%)	TOF (h^{-1})	Yield (%)	TOF (h^{-1})
L1	81.8 ± 2.5	528 ± 6	76.0 ± 12.1	96 ± 3	63.2 ± 2.9	95 ± 5	24.1 ± 3.5	166 ± 24
L2	81.0 ± 1.0	505 ± 27	85.3 ± 1.9	203 ± 9	71.2 ± 2.9	208 ± 2	39.7 ± 1.7	435 ± 52
L3	71.5 ± 0.5	8.7 ± 0.5	37.9 ± 4.0	2 ± 1	35.7 ± 2.7	3 ± 2	22.4 ± 2.7	44 ± 10
L7	61.9 ± 3.0	9.1 (lit)	40.8 ± 9.1	3 ± 2	37.7 ± 19.2	3 ± 2	21.5 ± 4.1	41 ± 1
$Cu(OTf)_2$	78.75	2667					45.6 ± 0.7	2017 ± 840
blind			22.2 ± 0.8	2 ± 1	29.6 ± 3.8	3	15.9 ± 9.1	57 ± 27

Table 5
Summary of the various tested reaction conditions to elucidate the mechanism of copper-bispidine catalyzed aziridination reaction.

Complex	**Air**		**O_2**	
	Yield (%)	TOF (h^{-1})	Yield (%)	TOF (h^{-1})
$[L1Cu^{II}](OTf)_2$	34.8 ± 9.2	16 ± 15	44.8 ± 3.6	> 27
	BHT		**TEMPO**	
	Yield (%)	TOF (h^{-1})	Yield (%)	TOF (h^{-1})
$[L1Cu^{I}]OTf$	0	120 ± 0	34.92 ± 2.5	13 ± 0
$[L1Cu^{II}](OTf)_2$	0	37 ± 2	28.9 ± 8.5	36 ± 3
	cis-Stilbene		**trans-β-Methylstyrene**	
	Yield (%)	TOF (h^{-1})	Yield (%)	TOF (h^{-1})
$[L1Cu^{II}](OTf)_2$	70.4 ± 9.5 (cis/trans 40/60)	80 ± 0	47.1 ± 0	40 ± 0

Due to the mixed product formation of 2,3-diphenyl-1-tosylaziridine from cis-stilbene it can be conclude that the NTs transfer occurs stepwise to the olefine. In the first step the double bond interacts with the nitrene leading to a C − C single bond intermediate which allows rotation and thus forming of the thermodynamic more stable trans product. In the second step the three membered ring gets closed forming the final aziridine. As only approximately 60 % of the formed aziridine undergoes the isomerization a short living intermediate is proposed and thus supporting the proposed radical character of the deprotonated copper nitrene species.

The radical character was further supported by a second set of experiments. For this purpose, radical scavengers such as tert-butylhydroxytoluene (BHT) or 2,2,6,6-tetramethylpiperidine-1-oxyl (TEMPO) were added to the reaction mixture. When equimolar amounts of BHT relative to PhINTs were used, no yield was obtained, and the time until the reaction solution cleared significantly increased, with a theoretical TOF of 120 h^{-1} for $[Cu^{I}L1]^{+}$ and 37 h^{-1} for $[Cu^{II}L1]^{2+}$. With TEMPO a significant decline was also observed, however, a yield of about 30 % was still achieved. But, since both radical quenchers have effects on the yield and TOF, these experiments further confirm a radical Cu(II)-nitrene species.

With all the previously described experiments combined, we are now able to clarify and correct different aspects of the catalytic cycle proposed in Bleher et al. [23] The reaction with $[CuL1]^{2+}$ proceeds via a Cu (I) species, which is formed by electron transfer from PhINTs to the Cu

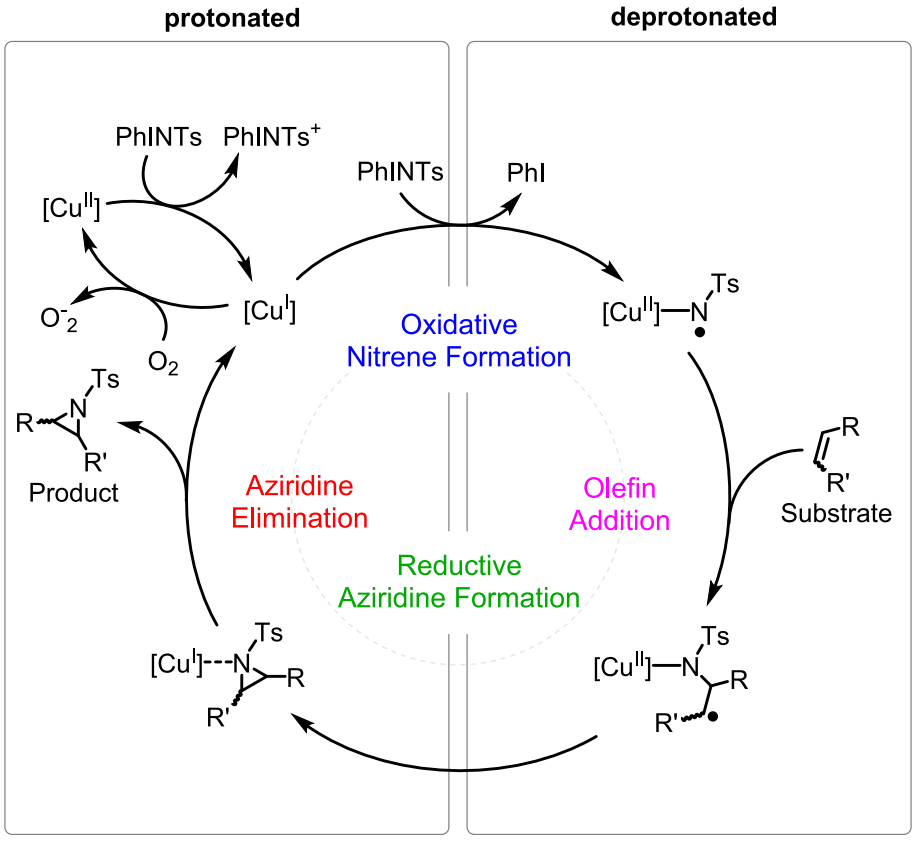

Fig. 7. Resulting reaction mechanism incorporating all information obtained from the experiments for $[CuL1]^{2+}$.

(II) precursor. The Cu(I) species is oxidized to the active nitrene complex with another equivalent of PhINTs, but can also be easily re-oxidized by atmospheric oxygen, consuming thereby oxidant unproductively. The formed copper(II)-nitrene species exhibits a radical character, leading to a stepwise conversion of substrates, resulting in the loss of stereochemical information. In contrast to many other copper-based complexes, the secondary amine positioned trans to the nitrene group plays a crucial role, as it was demonstrated by adding base and acid to the reaction solution. The reversible deprotonation in trans position of the nitrene group leads to a change in the nitrene's character through the direct interaction of the involved orbitals, which accelerates the catalytic cycle and results in higher TOFs and yields. The resulting mechanism is illustrated in Fig. 7.

4. Conclusion

We have demonstrated that the introduction of a secondary amine into the bispidine scaffold trans to the coordinating nitrene group increases the TOF in the copper-catalyzed aziridination of styrene. This is made possible by a reversible deprotonation that occurs during the progression of the reaction mechanism, which shifts the nitrene character towards a radical triplet nitrene, thereby increasing reactivity. Therefore, by adding small amounts of bases, the deprotonation equilibrium can be shifted, thus further tuning the reaction rates. Based on the observations made here, incorporating of secondary amines into similar catalysts could be a promising tool to increase the catalytic activity also beside from copper-catalyzed aziridination. It would also be interesting to examine whether the pKa value of the secondary amines correlates with the reactivity of the individual complexes. This aspect could offer further insights into the relationship between the ligand's electronic properties and its catalytic performance. Additionally, we were able to show that for the bispidine-based complex studied here, the corresponding Cu(II)-nitrene species exhibit a radical character, leading to a stepwise substrate conversion without preserving stereo information. Moreover, in the course of the experiments conducted to study the reaction mechanism, we were able to directly detect a bispidine-Cu-nitrene species for the first time using mass spectrometry, further supporting the proposed mechanism.

Declaration of competing interest

The authors declare that they have no known competing financial interests or personal relationships that could have appeared to influence the work reported in this paper.

Acknowledgments

We would like to express our gratitude to Matthias Franzreb and Peter Comba for granting us access to their laboratories and for offering valuable insights during the preparation of this manuscript. This research did not receive any specific grant from funding agencies in the public, commercial, or not-for-profit sectors.

Appendix A. Supplementary data

Supplementary data to this article can be found online at https://doi.org/10.1016/j.ica.2025.122587.

Data availability

Data will be made available on request.

References

[1] T. Rogge, N. Kaplaneris, N. Chatani, J. Kim, S. Chang, B. Punji, L.L. Schafer, D. G. Musaev, J. Wencel-Delord, C.A. Roberts, R. Sarpong, Z.E. Wilson, M.A. Brimble, M.J. Johansson, L. Ackermann, C–H activation (2021), https://doi.org/10.1038/s43586-021-00041-2.
[2] C. Dank, L. Ielo, Recent advances in the accessibility, synthetic utility, and biological applications of aziridines, Org. Biomol. Chem. 21 (2023) 4553–4573, https://doi.org/10.1039/d3ob00424d.
[3] R.T. Gephart, T.H. Warren, Copper-catalyzed sp3 C−H amination, Organometallics 31 (2012) 7728–7752.
[4] G. Dequirez, V. Pons, P. Dauban, Nitrene chemistry in organic synthesis: still in its infancy? Angew. Chem. Int. Ed. 51 (2012) 7384–7395, https://doi.org/10.1002/anie.201201945.
[5] A.K. Yudin, Aziridines and Epoxides in Organic Synthesis, John Wiley & Sons, 2006.
[6] J.B. Sweeney, Aziridines: Epoxides' ugly cousins? Chem. Soc. Rev. 31 (2002) 247–258, https://doi.org/10.1039/b006015l.
[7] H. Kwart, A.A. Kahn, Copper-catalyzed decomposition of Benzenesulfonyl Azide in cyclohexene solution, JACS 89 (1967) 1951–1953.
[8] D.A. Evans, M.M. Faul, M.T. Bilodeau, Copper-catalyzed Aziridination of olefins by (N-(p-Toluenesulfonyl)imino)phenyliodinane, J. Organomet. Chem. 56 (1991) 6744–6746.
[9] D.A. Evans, M.M. Faul, M.T. Bilodeau, Development of the copper-catalyzed olefin Aziridination reaction, J. Am. Chem. Soc. 116 (1994) 2742–2753.
[10] S. Liang, M.P. Jensen, Half-sandwich scorpionates as nitrene transfer catalysts, Organometallics 31 (2012) 8055–8058, https://doi.org/10.1021/om3009102.
[11] K.L. Klotz, L.M. Slominski, A.V. Hull, V.M. Gottsacker, R. Mas-Ballesté, L. Que, J. A. Halfen, Non-heme iron(II) complexes are efficient olefin aziridination catalysts, Chem. Commun. 114 (2007) 2063–2065, https://doi.org/10.1039/b700493a.
[12] I. Monte-Pérez, S. Kundu, K. Ray, An open-shell spin singlet copper-nitrene intermediate binding redoxinnocent metal ions: influence of the Lewis acidity of the metal ions on spectroscopic and reactivity properties, Zeitschrift Fur Anorg. Und Allg, Chemie 641 (2015) 78–82, https://doi.org/10.1002/zaac.201400389.
[13] J.A. Halfen, J.K. Hallman, J.A. Schultz, J.P. Emerson, Remarkably efficient olefin aziridination mediated by a new copper(II) complex, Organometallics 18 (1999) 5435–5437, https://doi.org/10.1021/om9908579.
[14] T. Uchida, T. Katsuki, Asymmetric nitrene transfer reactions: Sulfimidation, aziridination and C-H amination using azide compounds as nitrene precursors, Chem. Rec. 14 (2014) 117–129, https://doi.org/10.1002/tcr.201300027.
[15] T. Josephy, R. Kumar, K. Bleher, F. Röhs, T. Glaser, G. Rajaraman, P. Comba, Synthesis, characterization, and reactivity of Bispidine-Iron(IV)-Tosylimido species, Inorg. Chem. (2024), https://doi.org/10.1021/acs.inorgchem.4c01237.
[16] H.J. Dequina, C.L. Jones, J.M. Schomaker, Recent updates and future perspectives in aziridine synthesis and reactivity, Chem 9 (2023) 1658–1701, https://doi.org/10.1016/j.chempr.2023.04.010.
[17] J. Moegling, A. Hoffmann, F. Thomas, N. Orth, P. Liebhäuser, U. Herber, R. Rampmaier, J. Stanek, G. Fink, I. Ivanović-Burmazović, S. Herres-Pawlis, Designed to react: terminal copper Nitrenes and their application in catalytic C−H aminations, Angew. Chem. Int. Ed. 57 (2018) 9154–9159, https://doi.org/10.1002/anie.201713171.
[18] R. Trammell, K. Rajabimoghadam, I. Garcia-Bosch, Copper-promoted functionalization of organic molecules: from biologically relevant cu/O 2 model systems to organometallic transformations, Chem. Rev. 119 (2019) 2954–3031, https://doi.org/10.1021/acs.chemrev.8b00368.
[19] F. Thomas, M. Oster, F. Schön, K.C. Göbgen, B. Amarouch, D. Steden, A. Hoffmann, A new generation of terminal copper nitrenes and their application in aromatic C-H amination reactions, Dalton Trans. 50 (2021) 6444–6462, https://doi.org/10.1039/d1dt00832c.
[20] L. Maestre, W.M.C. Sameera, M.M. Díaz-Requejo, F. Maseras, P.J. Pérez, A general mechanism for the copper- and silver-catalyzed olefin aziridination reactions: concomitant involvement of the singlet and triplet pathways, J. Am. Chem. Soc. 135 (2013) 1338–1348, https://doi.org/10.1021/ja307229e.
[21] P. Brandt, M.J. Södergren, P.G. Andersson, P.O. Norrby, Mechanistic studies of copper-catalyzed alkene aziridination, J. Am. Chem. Soc. 122 (2000) 8013–8020, https://doi.org/10.1021/ja993246g.
[22] Y. Ren, K. Cheaib, J. Jacquet, H. Vezin, L. Fensterbank, M. Orio, S. Blanchard, M. Desage-El Murr, Copper-catalyzed Aziridination with redox-active ligands: molecular spin catalysis, Chem. - A Eur. J. 24 (2018) 5086–5090, https://doi.org/10.1002/chem.201705649.
[23] K. Bleher, P. Comba, M. Gast, S. Kronenberger, T. Josephy, Copper-bispidine-catalyzed aziridination – a new twist in small molecule activation, Inorg. Chim. Acta 532 (2022) 120752, https://doi.org/10.1016/j.ica.2021.120752.
[24] A.I.O. Suarez, V. Lyaskovskyy, J.N.H. Reek, J.I. Van Der Vlugt, B. De Bruin, Complexes with nitrogen-centered radical ligands: classification, spectroscopic features, reactivity, and catalytic applications, Angew. Chem. Int. Ed. 52 (2013) 12510–12529, https://doi.org/10.1002/anie.201301487.
[25] P.F. Kuijpers, J.I. . van der Vlugt, S. Schneider, B. de Bruin, Nitrene radical intermediates in catalytic synthesis, Chem. - A Eur. J. 23 (2017) 13819–13829, https://doi.org/10.1002/chem.201702537.
[26] Y. Guo, C. Pei, R.M. Koenigs, A combined experimental and theoretical study on the reactivity of nitrenes and nitrene radical anions, Nat. Commun. 13 (2022) 1–10, https://doi.org/10.1038/s41467-021-27687-6.
[27] M. Ju, J.M. Schomaker, et al., Nat. Rev. Chem. 5 (2021) 580–594, https://doi.org/10.1038/s41570-021-00291-4.
[28] M.E. Harvey, D.G. Musaev, J. Du Bois, A diruthenium catalyst for selective, intramolecular allylic C-H amination: reaction development and mechanistic insight gained through experiment and theory, J. Am. Chem. Soc. 133 (2011) 17207–17216, https://doi.org/10.1021/ja203576p.

[29] C. Weatherly, J.M. Alderson, J.F. Berry, J.E. Hein, J.M. Schomaker, Catalyst-Controlled Nitrene Transfer by Tuning Metal:Ligand Ratios: Insight into the Mechanisms of Chemoselectivity, Organometallics 36 (2017) 1649–1661, https://doi.org/10.1021/acs.organomet.7b00190.
[30] G. Parkin, Synthetic analogues relevant to the structure and function of zinc enzymes, Chem. Rev. 104 (2004) 699–767, https://doi.org/10.1021/cr0206263.
[31] I. Kampatsikas, A. Rompel, Similar but still different: which amino acid residues are responsible for varying activities in type-III copper enzymes? ChemBioChem 22 (2021) 1161–1175, https://doi.org/10.1002/cbic.202000647.
[32] P. Comba, M. Morgen, H. Wadepohl, Tuning of the properties of transition-metal bispidine complexes by variation of the basicity of the aromatic donor groups, Inorg. Chem. 52 (2013) 6481–6501, https://doi.org/10.1021/ic4004214.
[33] C. Mannich, P. Mohs, Über Derivate eines aus zwei Piperidinringen kondensierten bicyclischen Systems, Chem. Ber. B 63 (1930) 608–612.
[34] P. Comba, L. Grimm, C. Orvig, K. Rück, H. Wadepohl, Synthesis and coordination chemistry of Hexadentate Picolinic acid based Bispidine ligands, Inorg. Chem. 55 (2016) 12531–12543, https://doi.org/10.1021/acs.inorgchem.6b01787.
[35] R. Haller, H. Unholzer, Substituiette 3,7-Diaza-bicyclo-[3,3,1]-nonanole-(9), Arch. Pharm. 304 (1971) 654–659.
[36] U. Holzgrabe, E. Erciyas, Synthese und Stereochemie potentiell stark analgetischer 2,4-rn-diarylsubstituierter 3,7-Diazabicyclo[3.3.L]nonan-9-on-1,5-diester, Arch. Pharm. 325 (1992) 657–663.
[37] H. Börzel, P. Comba, K.S. Hagen, C. Katsichtis, H. Pritzkow, A copper(I) oxygenation precursor in the entatic state: two isomers of a copper(I) compound of a rigid tetradentate ligand, Chem. - A Eur. J. 6 (2000) 914–919, https://doi.org/10.1002/(sici)1521-3765(20000303)6:5<914::aid-chem914>3.0.co;2-k.
[38] Y. Yamada, T. Yamamoto, M. Okawara, Synthesis and reaction of new type i–n ylide, n-tosyliminoiodinane, Chem. Lett. 4 (1975) 361–362, https://doi.org/10.1246/cl.1975.361.
[39] F. Bruchertseifer, P. Comba, B. Martin, A. Morgenstern, J. Notni, M. Starke, H. Wadepohl, First-generation Bispidine chelators for 213BiIII radiopharmaceutical applications, ChemMedChem 15 (2020) 1591–1600, https://doi.org/10.1002/cmdc.202000361.
[40] P. Comba, M. Starke, H. Wadepohl, Optimization of Hexadentate Bispidine ligands as chelators for 64CuII PET imaging, Chempluschem 83 (2018) 597–604, https://doi.org/10.1002/cplu.201800110.
[41] K. Born, P. Comba, R. Ferrari, G.A. Lawrance, H. Wadepohl, Stability constants: a new twist in transition metal bispidine chemistry, Inorg. Chem. 46 (2007) 458–464, https://doi.org/10.1021/ic061501+.
[42] P. Comba, S. Fukuzumi, C. Koke, B. Martin, A.M. Löhr, J. Straub, A Bispidine Iron (IV)–Oxo complex in the Entatic state, Angew. Chem. Int. Ed. 55 (2016) 11129–11133, https://doi.org/10.1002/anie.201605099.
[43] P. Comba, C.L. De Laorden, H. Pritzkow, Tuning the properties of copper(II) complexes with tetra- and pentadentate bispidine (= 3,7-diazabicyclo[3.3.1]nonane) ligands, Helv. Chim. Acta 88 (2005) 647–664, https://doi.org/10.1002/hlca.200590045.
[44] R. Gleiter, M. Kobayashi, J. Kuthan, The n-orbital sequence in 1,3 diazaadamantane, Tetrahedron 32 (1976) 2775–2781, https://doi.org/10.1016/0040-4020(76)80122-6.
[45] P. Comba, A. Hauser, M. Kerscher, H. Pritzkow, Bond-stretch isomerism: trapped isomeric structures of hexacoordinate copper(II) bispidine chromophores along a Jahn-teller active vibrational coordinate, Angew. Chem. Int. Ed. 42 (2003) 4536–4540, https://doi.org/10.1002/anie.200351900.
[46] P. Paoletti, L. Fabbrizzi, R. Barbucci, Thermochemistry of metal-polyamine complexes, Inorganica Chim. Acta Rev. 7 (1973) 43–68, https://doi.org/10.1016/0073-8085(73)80164-0.
[47] A.R. Rossi, R. Hoffmann, Transition Metal Pentacoordination, Inorg. Chem. 14 (1975) 365–374, https://doi.org/10.1021/ic50144a032.
[48] M. Duggan, N. Ray, B. Hathaway, G. Tomlinson, Paul Brint, K. Pelin, Crystal structure and electronic properties of ammine[tris(2-amino- ethyl)amine]copper (i−) Diperchlorate and potassium Penta-ammine- copper, J.C.S. Dalt. (1980) 1342–1348.
[49] C. Schneider, Synthese und Charakterisierung neuer Bispidin-Liganden und ihrer Metallkomplexe für die potentielle Anwendung in der Nuklearmedizin, 2015.
[50] P. Comba, M. Merz, H. Pritzkow, Catalytic aziridination of styrene with copper complexes of substituted 3,7-Diazabicyclo[3.3.1]nonanones, Eur. J. Inorg. Chem. (2003) 1711–1718, https://doi.org/10.1002/ejic.200200618.
[51] M. Abu-Odeh, K. Bleher, N. Johnee Britto, P. Comba, M. Gast, M. Jaccob, M. Kerscher, S. Krieg, M. Kurth, Pathways of the extremely reactive Iron(IV)-oxido complexes with Tetradentate Bispidine ligands, Chem. - A Eur. J. 27 (2021) 11377–11390, https://doi.org/10.1002/chem.202101045.
[52] P. Comba, C. Lang, C.L. De Laorden, A. Muruganantham, G. Rajaraman, H. Wadepohl, M. Zajaczkowski, The mechanism of the (bispidine)copper(ii)-catalyzed aziridination of styrene: a combined experimental and theoretical study, Chem. - A Eur. J. 14 (2008) 5313–5328, https://doi.org/10.1002/chem.200701910.